ACS OMEGA

http://pubs.acs.org/journal/acsodf

Article

Investigation of Asian Dyes and Pigments from the Artifact of "Murongzhi" and the Silk Road in China

Yanfei Wei, Wenting Gu, Lei Zhong, Bingbing Liu, Feixiang Huang, Yuhua Chang, Mingke Li, Yaya Jing, and Guoke Chen*

Cite This: *ACS Omega* 2023, 8, 2508−2519

Read Online

ACCESS | Metrics & More | Article Recommendations | Supporting Information

ABSTRACT: In this paper, a series of modern analysis methods, including Raman spectroscopy, X-ray diffraction, UV−vis spectrophotometry, and ultra-high-pressure liquid chromatography coupled with a thermoelectric LTQ-Orbitrap XL ETD mass spectrometer (UHPLC-MS/MS), were applied to analyze and accurately identify the chemical composition of plant dyes and the mineral pigment from the samples collected from grave goods. As a result, the textiles were dyed by the madder, Kermes, *Phellodendron chinense*, indigo, *Lithospermum* L., and so forth. In addition, the mineral pigment, charcoal, hematite, minium, cinnabar, azurite, and malachite were used to paint the exquisite artifacts in the tomb of Murongzhi. This research demonstrates the profound impact on cultural transmission and fusion in the "Tuyuhong" dynasty and explores the Silk Road in Tang dynasty.

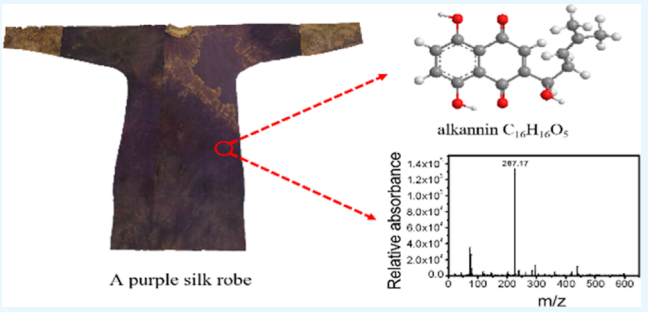

1. INTRODUCTION

The geographical origins of the Silk Road indirectly indicate that the most influential cultures, Hellenic, Islamic, and Indian-in Eurasia, all converged in China at Tang dynasty.[1,2] This vast network of trade routes linked China with Western countries, which facilitated an unprecedented increase in bidirectional communication, technology transfer, and human movement across Eurasia.[3,4] In addition to the economic trades,[5−8] a remarkably diverse array of ideas, religions, mining techniques, and cultigen were also introduced into ancient China from Eurasia.[9,10] Meanwhile, China transported silk and other goods to Western countries through the Silk Road during that period. In particular, as one of important symbols in the history of transportation, "Tuyuhun" was located in the main road of land transportation between China and the West on the Silk Road (Figure 1).

The tomb of Murongzhi has received much attention in recent years due to its important location on the middle branch of the Silk Road during the Tang dynasty of China. According to the unearthed epitaph, the cemetery can be dated to the second year of the Wuzhou era (691 AD), and the tomb occupant has been identified as Murongzhi, a member of the Tuyuhun royal family.[11,12] It is essential that a large number of well-preserved artifacts were unearthed, which has provided us with opportunities to study economic and cultural exchanges about Tuyuhun along the Silk Road. The representative artifacts in the tomb of Murongzhi are shown in Figure 2. The coffin was draped with an exquisite carpet, elaborately decorated with elephants in alignment that was colored blue (Figure 2a). The upper platform of the coffin was covered sequentially with a red carpet (Figure 2b). Those amazing carpets have indirectly reflected the high social or political status of Murongzhi. Closing to the corpse, it displays with a dark-purple silk robe elaborately embroidered with colorful threads (Figure 2c). Besides, due to the arid conditions in the Wuwei region of China, an array of exquisite artifacts have been preserved in the lavish tomb (Figure 2d−g), which is unprecedented and sets this tomb apart from others found in China from this region and time period. Tuyuhun is considered as a pearl of discoveries on the Silk Road and is of paramount importance in the field of oriental studies. The extremely dry environmental conditions permitted the exceptional preservation of the works of art present in the tomb, not only colorful mural paintings and pottery but also organic materials, such as lacquer wood, silk paintings, and textiles.[13] Among them, the dye and pigment of cultural relics were the representatives of the symbol of cultural exchange on the Silk Road. These provide information about the use of natural dyes and pigments during the Tuyuhun period.

With the help of newly developed analytical techniques, numerous studies identifying natural dyes and mineral pigments in archaeological sites have been carried out.[14−19] Therefore, in

Received: October 31, 2022
Accepted: December 14, 2022
Published: January 4, 2023

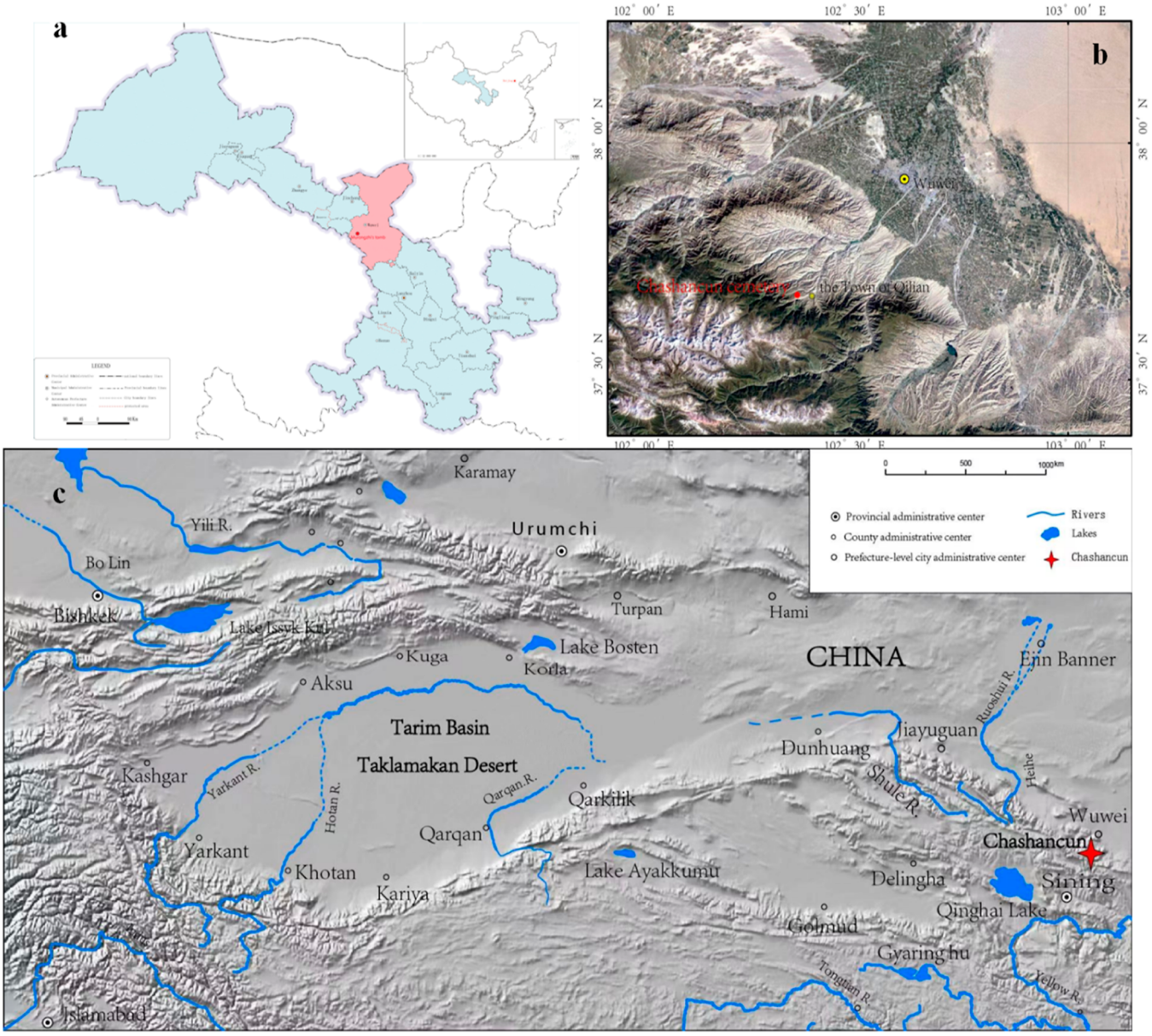

Figure 1. Maps a–c showing the location of Murongzhi cemetery (red symbol) in Wuwei of China.

this study, we used a number of multi-analytical scientific technologies, including X-ray diffraction (XRD) and micro-Raman spectroscopy (μ-Raman), to analyze pigments, and a UHPLC-DAD-MS, UV–vis spectrophotometer with mild extraction of dyes was used to characterize dyes from textiles.[20−26] The textile samples and the mineral pigment from cultural relics were analyzed. Based on the results, fiber materials, the origins of dyes (including plant species), and dyeing technologies were revealed. This work also demonstrates the profound impact and cultural fusion that the Silk Road had upon the people of Tuyuhong and Eurasia.

2. EXPERIMENTAL SECTION

2.1. Chemicals and Reagents. DMSO (chromatographically pure), concentrated hydrochloric acid (37%), methanol (chromatographically pure), acetonitrile (chromatographically pure), formic acid (chromatographically pure), and purified water were used in this study.

2.2. Apparatus. A super-depth-of-field microscope was used to observe the microscopic morphology of the sample. The detection instrument was a Japanese Keyence VHX-5000 super-depth-of-field three-dimensional microscope system, the detection environment is the indoor natural environment, and the lens is a Keyence VH-Z20R lens, with a magnification range of 20× to 200× and an observation distance of 25.5 mm. A CM-36d spectroscopic color meter was used to evaluate the color of textiles. The UV–vis spectra were tested on a Cary 500 Scan UV–vis absorption spectrophotometer (Varian, CA, USA). A powder XRD experiment equipped with a Rigaku D/Max 2550PC diffractometer operating with Cu Kα radiation (40 kV, 150 mA) at a scan rate of 8°/min in the range from 3 to 90° was carried to confirm the mineralogical compositions of surface pigments. The Raman spectrometer of Japan's HORIBA LabRAM HR Evolution was used to conduct laser Raman analysis on the samples; the excitation wavelength is 785 nm, the power is less than 300 MW, the spectral range is 50–2000 cm^{-1}, and the integration time is 10 s.

https://doi.org/10.1021/acsomega.2c06572
ACS Omega 2023, 8, 2508−2519

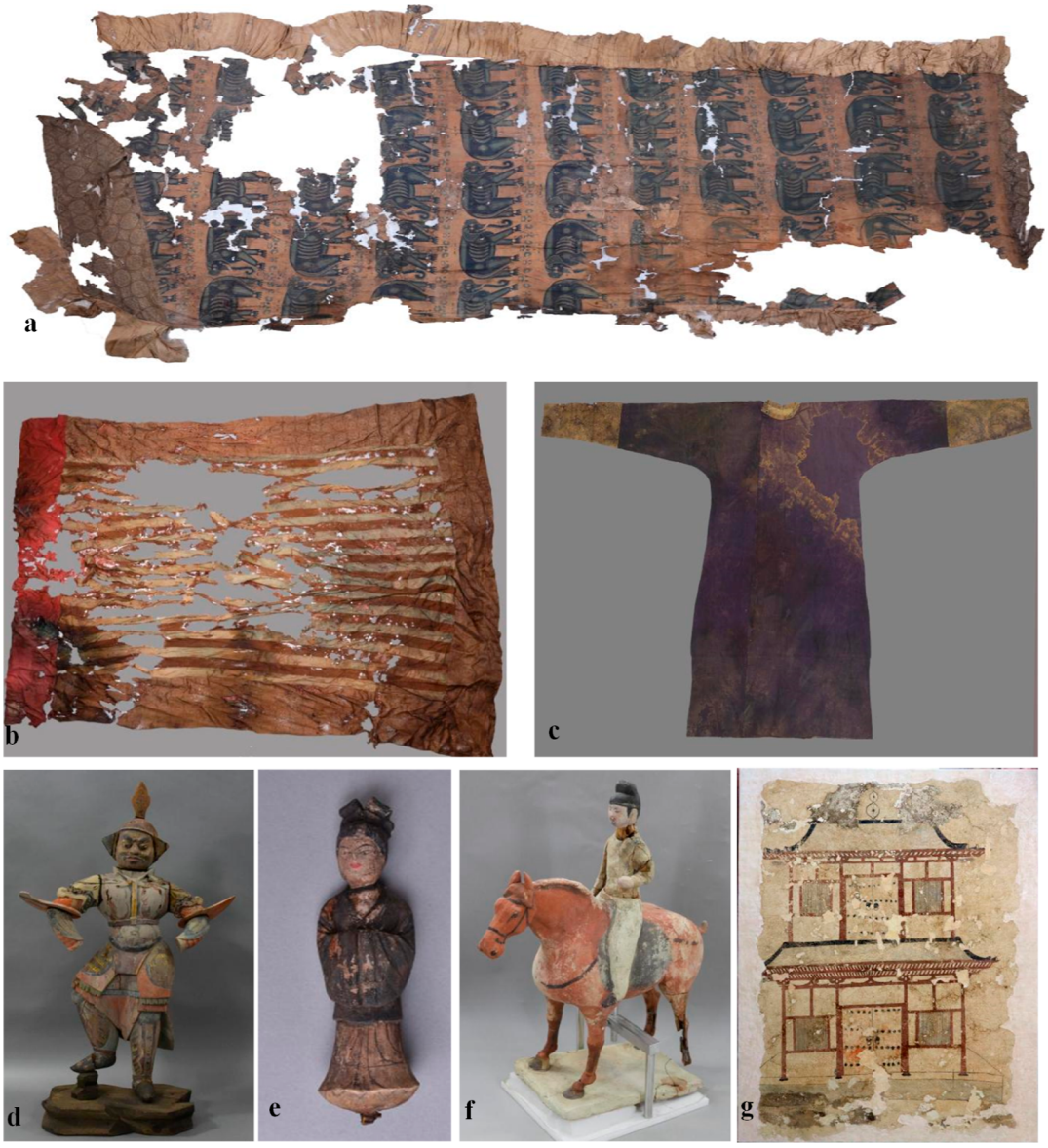

Figure 2. Artifacts of the tomb of Murongzhi. (a) Image of a carpet with decorative patterns of elephants; (b) image of a carpet with colored red stripes; (c) image of an elaborately embroidered dark-purple silk robe (c); and (d−g) images of an array of exquisite artifacts in the lavish tomb, painted lacquer wood ware (d), painted pottery (e), painted horse-riding figure (f), and mural (g).

A thermoelectric LTQ-Orbitrap Velos Orbitrap coupled with UHPLC, a USC-502 ultrasonic apparatus, a BUCHIR-215 rotary evaporator, a DK-S24 electric-heated thermostatic water bath, an ESJ200-4B analytical balance, an Eco KL-UP-III ultrapure water tester were used. In addition, the liquid chromatography conditions are as follows: analysis was carried out using UHPLC. Column parameters: Agilent Extend C_{18} UHPLC reversed-phase column (2.1 mm × 50 mm, 1.8 μm), column temperature 30 °C, flow rate 0.25 mL/min, and injection volume 1 μL; mobile phase: 0.1% formic acid aqueous solution in mobile phase A and acetonitrile solution in mobile phase B. Gradient elution program: at 0−9 min, the proportion of phase A decreased from 95 to 5%; at 9−10.3 min, the proportion of phase A was 5%; at 10.3−10.5 min, the proportion of phase A increased from 5 to 95%; and the detection wavelength was 280 nm. The electron spray ionization in the QTOF mode was used to collect the primary mass spectrometry data of the sample. Mass spectrometry: the optimized mass spectrometric parameters are as follows: atomization temperature: 350 °C, atomizer flow rate: 10 L/min, atomization pressure: 30 psig, capillary voltage: 7000 V, capillary outlet voltage: 150 V, and scanning range: 50−1000 amu. FT Full Scan was applied. Internal standard calibration: at m/z 112.9859 and 1033.9881, real-time quality correction was performed on analysis results. The collision voltage value of the target secondary ion mode (targeted MS/MS) was set as 20 and 30 eV according to the difficulty of fragmentation of the target ion.

2.3. Extraction and Sampling Procedures. All the samples of the textile were treated using the method published in the literature for stripping dyes.[13,14] The sample to be tested was added to 200 μL of DMSO solvent, the dye was dissolved in a 60 °C water bath, and the supernatant was extracted for use. Then, the hydrochloric acid method was used to fully dissolve the dye in the residue. The residue was added to 200 μL of 37% hydrochloric acid/methanol/water = 2:1:1 (v/v/v), heated in a 60 °C water bath for 60 min, filtered, and spin-dried with a rotary

https://doi.org/10.1021/acsomega.2c06572
ACS Omega 2023, 8, 2508−2519

Table 1. Microscopic Examination of Pigments and Fibers

Sample	Color	Magnified image	Sample source
1	Red fibers		textile
2	Yellow fibers		textile
3	Green fibers		textile
4	Purple fibers		textile
5	Blue fibers		textile
6	Red pigment	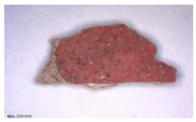	Painted pottery
7	Red pigment		mural
8	Nattier blue pigment		mural
9	Blue pigment	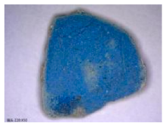	tomb-guardian
10	Orange pigment	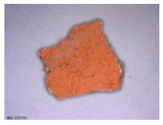	mural
11	Green pigment	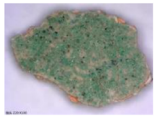	tomb-guardian

evaporator. Then, the supernatant extracted in the first step was mixed with the residue dried in the second step thoroughly under the action of ultrasound. Then, the mixture was centrifuged. Then, 20 μL of the supernatant was taken and injected into the chromatographic system for detection.

2.4. Method. First, we observed the pigment distribution and the color of textiles with a super-depth-of-field microscope and a spectroscopic color meter (Tables 1 and S1). In addition, we used UV−vis spectra to detect the peak of absorbance of the different extracts. Then, we combined UHPLC and high-resolution Q-TOF-MS to identify the organic dyes. Finally, we applied Raman spectroscopy and XRD to confirm the mineralogical compositions and the type of pigment, respectively.

3. RESULTS AND DISCUSSION

3.1. Dye Identification of the Textiles. The UV−vis curve is used as a function of wavelength (λ) of the different extracts to know at which λ the peak of absorbance appears. The peaks of

https://doi.org/10.1021/acsomega.2c06572
ACS Omega 2023, 8, 2508−2519

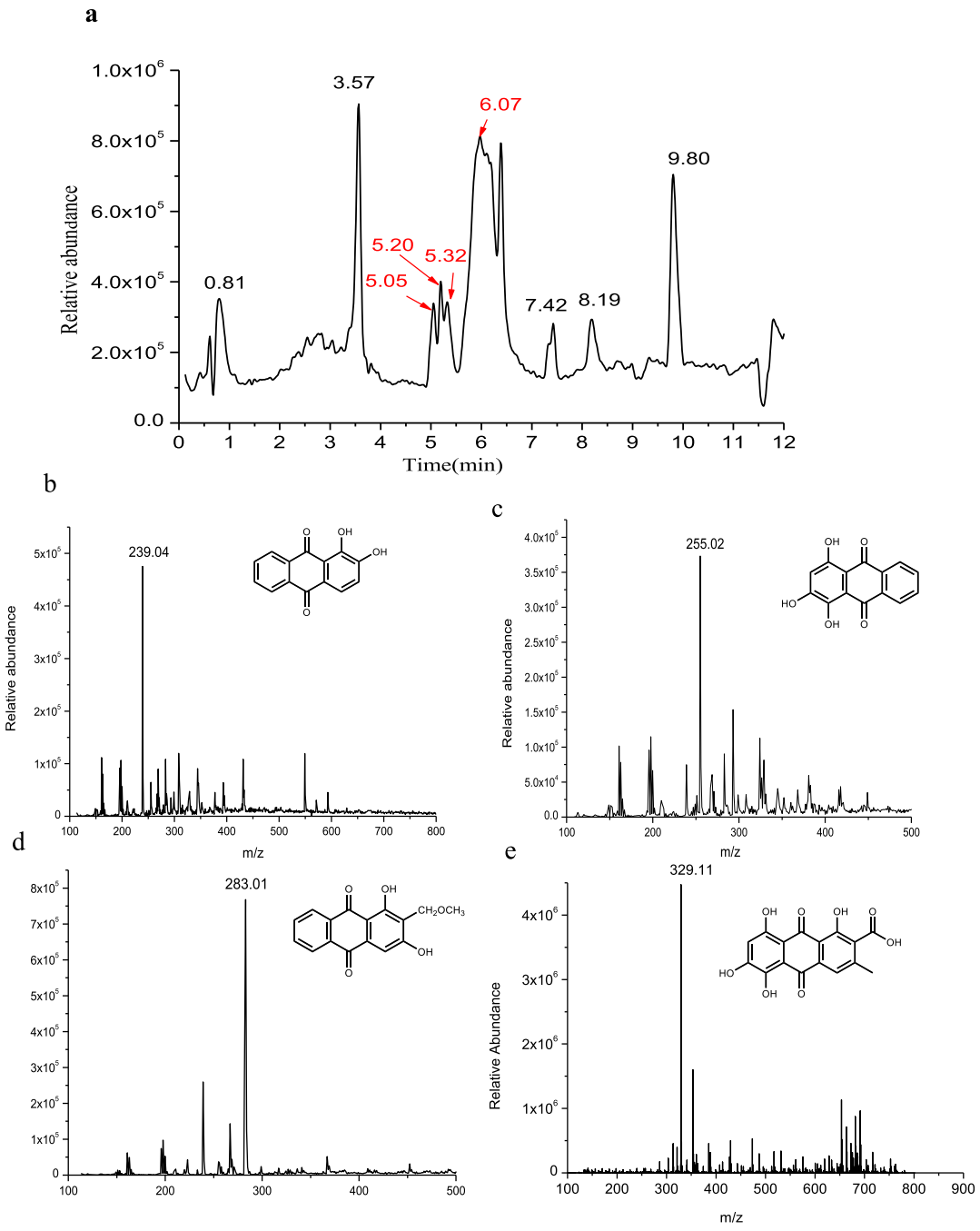

Figure 3. (a) UHPLC-Q-LTQ-Orbitrap total ion chromatogram in the red silk extract and (b−e) MS/MS spectra of the compounds *m*/*z* 239.04, *m*/*z* 255.02, *m*/*z* 283.02, and *m*/*z* 329.11 eluted in the UPLC peak at 5.19, 5.32, 6.07, and 5.05 min, respectively, in the red silk extract.

absorbance of the UV−vis curves of different colored dyes of textiles are shown in Figures S1−S5. The extracts of red fiber show the peak of absorbance near 262 nm (Figure S1); the extracts of yellow fiber show the peak of absorbance near 261 nm (Figure S2); the extracts of blue fiber show the peaks of absorbance near 261, 286, and 616 nm (Figure S3); the extracts of purple fiber shows the peaks of absorbance near 262 and 592 nm (Figure S4); and the extracts of green fiber shows the peaks of absorbance near 261, 284, and 615 nm (Figure S5).

Figure 3 shows the total ion current (Figure 3a) and the corresponding mass spectrum detected in the dye extract of the red textile sample. It can be seen from Figure 3b that the charge-to-mass ratio (*m*/*z*) of the molecular ion peak was 239.04 at a retention time of 5.20 min in the mass spectrum, which is consistent with the theoretical value 239.0390 of alizarin $C_{14}H_8O_4$. As shown in Figure 3c, the charge-to-mass ratio (*m*/*z*) of the molecular ion peak was 255.02 at a retention time of 5.32 min in the mass spectrum, which is the same as that of the fragment ion peak of purpurin $C_{16}H_{11}O_2N_2$. The charge-to-mass ratio (*m*/*z*) of the molecular ion peak was 283.02 at a retention time of 6.07 min in the mass spectrum (Figure 3d), which is consistent with the theoretical value 283.0601 of 1,3-dihydroxy-2-methoxy-anthraquinone $C_{14}H_8O_5$. The detected alizarin, purpurin, and 1,3-dihydroxy-2-methoxy-anthraquinone are the typical anthraquinones, which are the main ingredients of madder. Thus, it is verified that the red textile was dyed by madder. The earliest madder (*Rubia tinctorum* and *Rubia cordifolia*) seems to be found in cotton from Mohenjo-Daro in

https://doi.org/10.1021/acsomega.2c06572
ACS Omega 2023, 8, 2508−2519

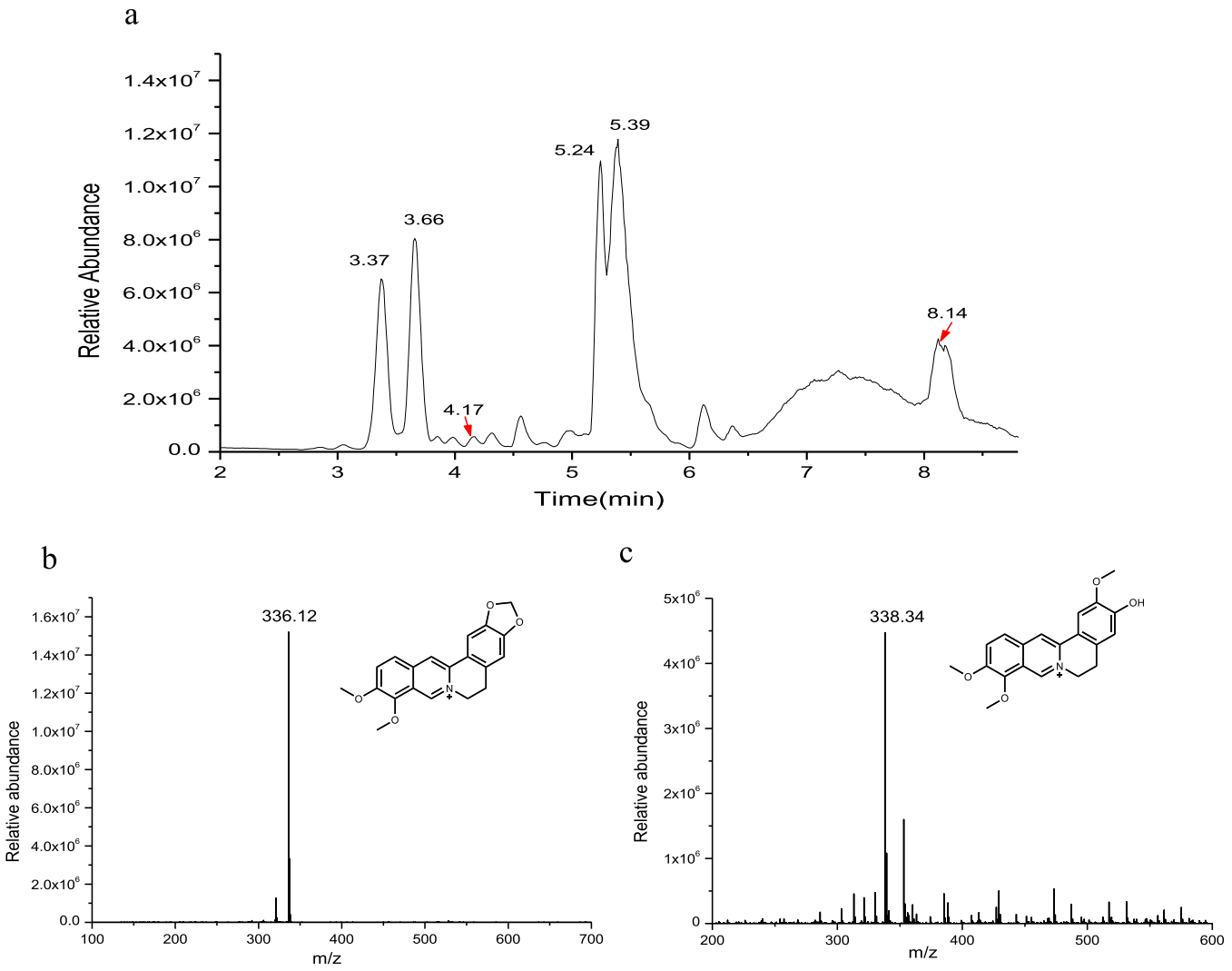

Figure 4. (a) UHPLC-Q-LTQ-Orbitrap total ion chromatogram in the yellow silk extract and (b,c) MS/MS spectra of the compound m/z 336.12 and m/z 338.34 eluted in the UPLC peak at 4.17 and 8.14 min, respectively.

the Indus Valley about 5000 years ago, which is a very common red dye grown in Europe and Central Asia.[27] As is well known, *R. cordifolia* contains large amounts of purpurin along with very small amounts of alizarin, whereas *R. tinctorum* has a very large alizarin peak.[28,29] Thus, it is inferred that the red textile has been dyed with *R. tinctorum* from the result of total ion current. *R. tinctorum* in South Asia may have been imported to the Central Plains through the route that passed through the Shu Kingdom (Sichuan Province of China).[30] In ancient China, madder has been the main red plant dye in "Shang" and "Zhou" dynasties.[31] In addition, madder had been planted widely in the Han dynasty in large quantities.[32] It was demonstrated that the impact of the culture of Eurasian steppes on the Tuyuhong culture was provided indirectly. It suggests that the transmission of dyestuffs from the Western Regions occurred around the second century BCE when the Silk Road was opened up.

In addition, one of the most intriguing findings in the present study is the identification of kermesic acid which was extracted from the red textile. Kermesic acid was discovered from Polish cochineal. The charge-to-mass ratio (m/z) of the molecular ion peak was 329.11 at a retention time of 5.05 min in the mass spectrum (Figure 3e), which was the same as that of kermesic acid $C_{16}H_{10}O_8$. Kermes originated from the dried bodies of female insects of the Kermes family that lived on Mediterranean prickly oak trees.[33,34] It is proposed that the presence of the plant dyes and insect dyes in Murongzhi textiles reflects the connections between the two cultures that had affected the Tuyuhun.[35]

Figure 4a shows the total ion current detected in the dye extract of the yellow textile sample. The charge-to-mass ratio (m/z) of the molecular ion peak was 336.1229 at a retention time of 4.17 min in the mass spectrum (Figure 4b), which was almost the same as the theoretical value 336.1232 of berberine $C_{20}H_{18}O_4N^+$. The charge-to-mass ratio (m/z) of the molecular ion peak was 338.3417 at a retention time of 8.14 min in the mass spectrum (Figure 4c), which was consistent with the theoretical value 338.1387 of jatrorrhizine $C_{20}H_{20}NO_4$.[36−39] Berberine and jatrorrhizine were detected in the yellow textile sample. Hence, we can conclude that the plant dye of yellow textile samples is *Phellodendron chinense*. The almost complete absence of palmatine can be taken as an indication of the possible use of *P. chinense* rather than *Phellodendron amurense*.[40,41] *P. chinense* is endemic in an area centered in the Western Hubei Province only about 200 km from Xi'an, which is at the eastern end of the Silk Road.[42,43]

https://doi.org/10.1021/acsomega.2c06572
ACS Omega 2023, 8, 2508−2519

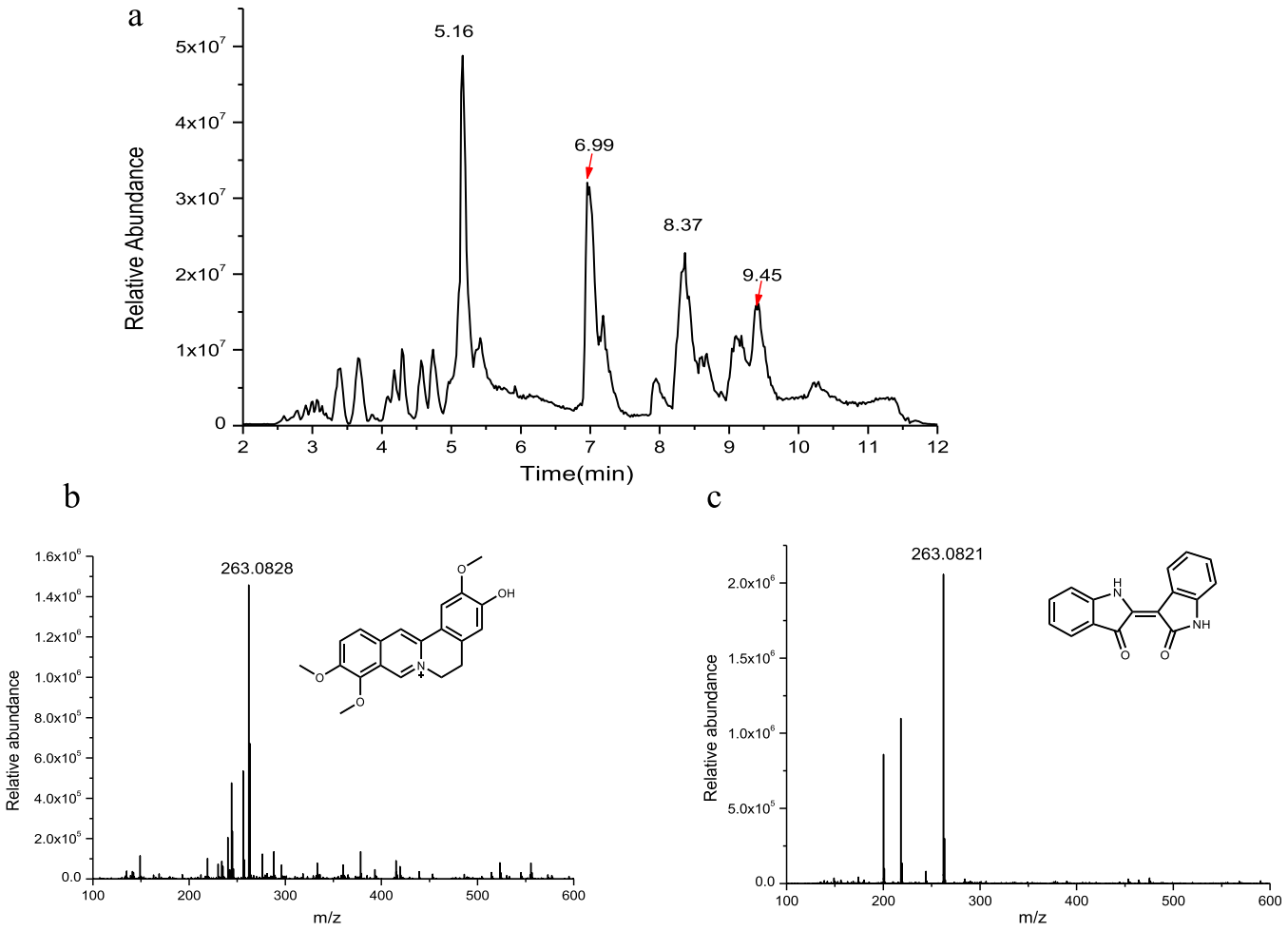

Figure 5. (a) UHPLC-Q-LTQ-Orbitrap total ion chromatogram in the blue silk extract and (b,c) MS/MS spectra of compounds m/z 263.08 and m/z 263.08 eluted in the UPLC peak at 6.99 and 9.45 min, respectively, in the blue silk extract.

According to the ion chromatogram (Figure 5a), the maximum chromatographic peak of the textile stripping dyes appeared at 6.99 min. The mass-to-charge ratio (m/z) was 263.0828 for the most abundant chromatographic peak, which was close to the theoretical value 263.0821 of indigo (Figure 5b). The mass-to-charge ratio (m/z) was 263.0827, which occurred at a retention time of 9.45 min, and the presence of indirubin in the sample is determined (Figure 5c).[44,45] Four important indigo-producing plants are *Strobilanthes cusia*, *Polygonum tinctorium*, *Indigofera tinctoria*, and *Isatis tinctoria*. The indigo and indirubin content will vary with the season of planting and harvest and the method of making indigo.[46] Archaeological evidence indicates that indigo was used to color cotton on the north coast of Peru as early as about 4000 BCE.[47]

The total ion current and the corresponding mass spectra of the dye extract of the purple textile sample are shown in Figure 6a. The charge-to-mass ratio (m/z) of the molecular ion peak was 287.17 at a retention time of 6.69 min in the mass spectrum (Figure 6b), which was consistent with the theoretical value 287.0919 of alkannin $C_{16}H_{16}O_5$. The charge-to-mass ratio (m/z) of the molecular ion peak was 329.26 at a retention time of 4.43 min in the mass spectrum, as shown in Figure 6c. Its molecular formula was $C_{18}H_{18}O_6$, which was exactly the same as that of the fragment ion peak of acetylshikonin. The molecular marker of Boraginaceae plants is shikonin.[48,49] It is deduced that the purple textile samples are dyed with *Lithospermum* L.[50] Boraginaceae plant is the most common source of purple in Asia.[51] It had become popular as early as the spring and autumn periods.

Large amounts of berberine ($[M + H]^+ = m/z$ 336) were detected in the green silk yarns, suggesting that *P. chinense* was probably the plant source of the dye used to color the silk textiles. The total ion current and the corresponding mass spectra of the dye extract of the green textile sample are shown in Figure 7a. The charge-to-mass ratio (m/z) of the molecular ion peak was 336.1229 at a retention time of 4.17 min in the mass spectrum (Figure 7b). Its molecular formula was $C_{20}H_{18}O_4N^+$, which was exactly the same as the fragment ion peak of berberine. The charge-to-mass ratio (m/z) of the molecular ion peak was 338.3412 at a retention time of 8.14 min in the mass spectrum (Figure 7c). Its molecular formula was $C_{20}H_{20}O_4N_4$, which was exactly the same as the fragment ion peak of jatrorrhizine. The large amounts of berberine were detected in green silk yarns, suggesting that *P. chinense* (from central China) was probably the plant source of the dye used to color the silk textiles. Therefore, it is inferred that the green textile sample contains yellow dye.[52] In addition, a molecular ion peak of m/z 263.0814 was detected in the green textile dye liquor extract, and its fragment ion peak was exactly the same as the indigo fragment ion peak (Figure 7d).[53,54] Therefore, it is deduced that the green textile samples were chromatically dyed with *P. chinense* and indigo. According to the analysis of experimental data, it is

https://doi.org/10.1021/acsomega.2c06572
ACS Omega 2023, 8, 2508−2519

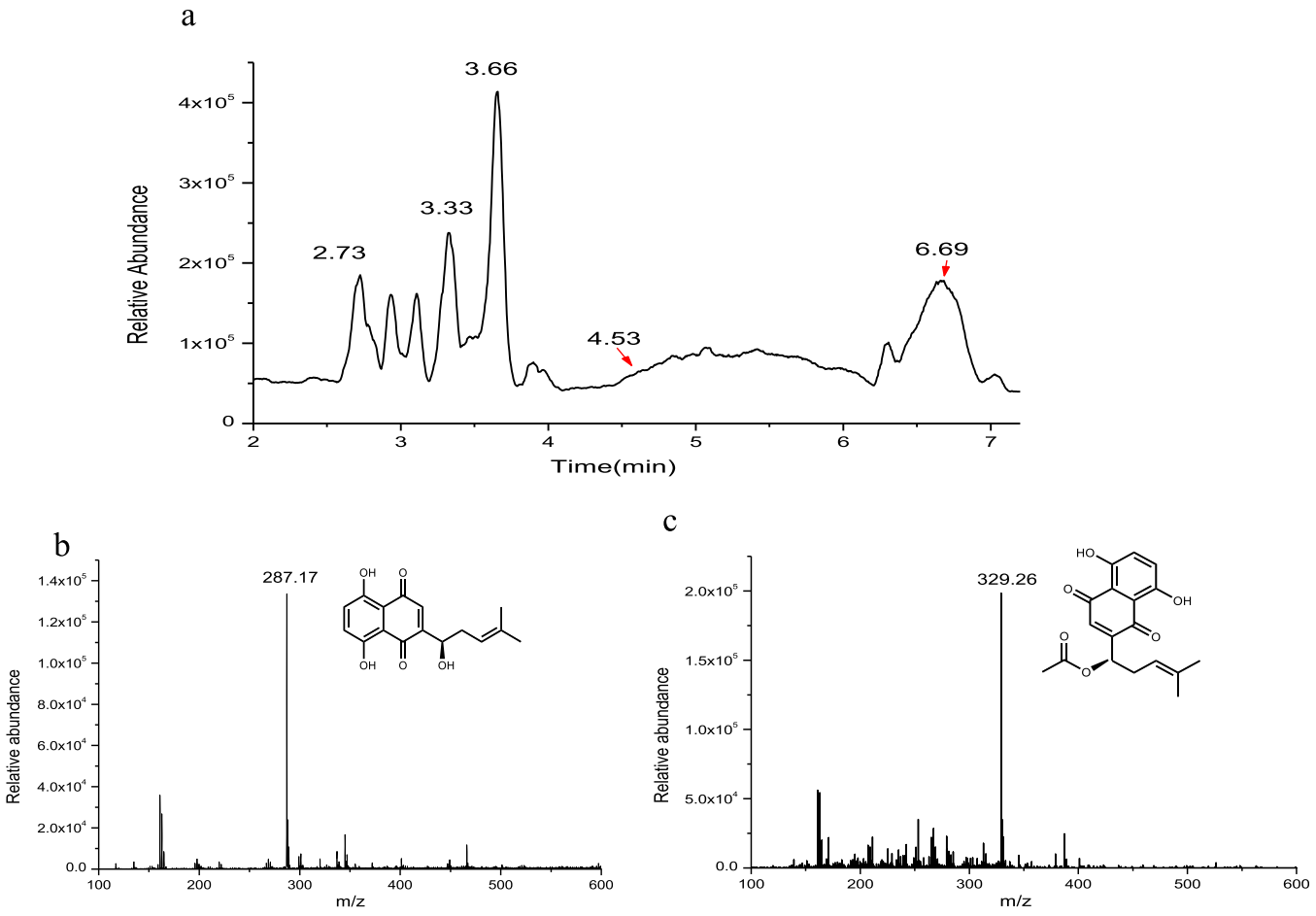

Figure 6. (a) UHPLC-Q-LTQ-Orbitrap total ion chromatogram in the purple silk extract and (b,c) MS/MS spectra of compounds *m*/*z* 287.17 and *m*/*z* 329.26 eluted in the UPLC peak at 6.69 and 4.43 min, respectively.

inferred that the green textiles were dyed chromatically with *P. chinense* and indigo. Moreover, the colorimetric evaluation of dyed samples (K/S; *L**, *a**, *b**) is discussed in Table S1. In addition, the corresponding content is given in the Supporting Information.

With the development of the Silk Road, many Western dyes were introduced into China, and the manufacturing process of dyeing was also mastered. In ancient China, madder has been the main red plant dye that could be used to dye textiles.[55] The textiles were dyed with madder and then mordanted with alum to get red color. In addition, Kermes were discovered to dye red textiles in this paper. *P. chinense* which are natural alkaloid pigments and have good dyeing effects on protein fibers could be used to dye the textile directly.[56] The blue textile samples were dyed with natural indigo and mainly through reduction dyeing to color textiles.[57] The green textile could be first dyed with Phellodendron and then chromatically dyed with indigo according to the literature.[50] *Lithospermum* L. is a very ancient vegetable dye. The root of *Lithospermum* L. contains shikonin, which can be mordant dyed with alum to get purple color.[58]

3.2. Mineralogical Compositions. Mineral pigments have become the most common basic pigments used by ancient artists in many countries, such as Egypt, India, China, and so forth.[59] Egyptians have been manufacturing pigments since about 4000 BC and were the main discoverers and contributors of mineral pigments.[60] Hematite and cinnabar are the main sources of red pigments. Lapis lazuli and azurite can be the main source of cyan pigments, and some also use indigo as the plant dye. In addition, Egyptians extracted malachite as the green pigment.[59]

Here, Raman spectroscopy and XRD were used to reveal the inorganic components of the pigment used in mural, terracotta, lacquer wood, and even textile in the tomb of Murongzhi. The Raman peaks of the red pigment of murals and pottery at 215, 287, 404^{-}, and 1323 cm^{-1} are consistent with that of hematite (Fe_2O_3) reference (Figure 8a). In addition, the strong diffraction peaks of the sample at 2θ of 29.8 and 39.8 are consistent with the diffraction peaks of hematite (Fe_2O_3) and lepidocrocite [FeO(OH)], respectively (Figure 8b). Therefore, it can be inferred that the red pigment should be hematite (Fe_2O_3). The Raman peaks of the orange pigment at 76.00, 138.48, 224.14, 472.76, and 541.28 cm^{-1} are basically consistent with the Raman peaks of minium (Pb_3O_4) reference (Figure 8c). In addition, the diffraction peaks of the sample at 2θ of 25.22, 26.84, 34.38, 34.83, 47.9, 49.54, and 52.54 are consistent with those of minium (Pb_3O_4) reference (Figure 8d), indicating that there are minium references in the surface layer. In addition, the Raman peaks of the dark red pigment found in the painting process in the textile at 248.5 (vs) and 341 (m) cm^{-1} are consistent with the Raman peaks of cinnabar (HgS) reference (Figure 8e). In addition, the strong diffraction peaks of the sample at 2θ of 27.04 and 31.64 are consistent with the diffraction peaks of hematite (HgS) (Figure 8f). In the Tang dynasty, with the expansion of human activities, more hematite materials were discovered.[61] Iron red was a pigment produced locally at that period. Compared with other red pigments, such as minium and

https://doi.org/10.1021/acsomega.2c06572
ACS Omega 2023, 8, 2508−2519

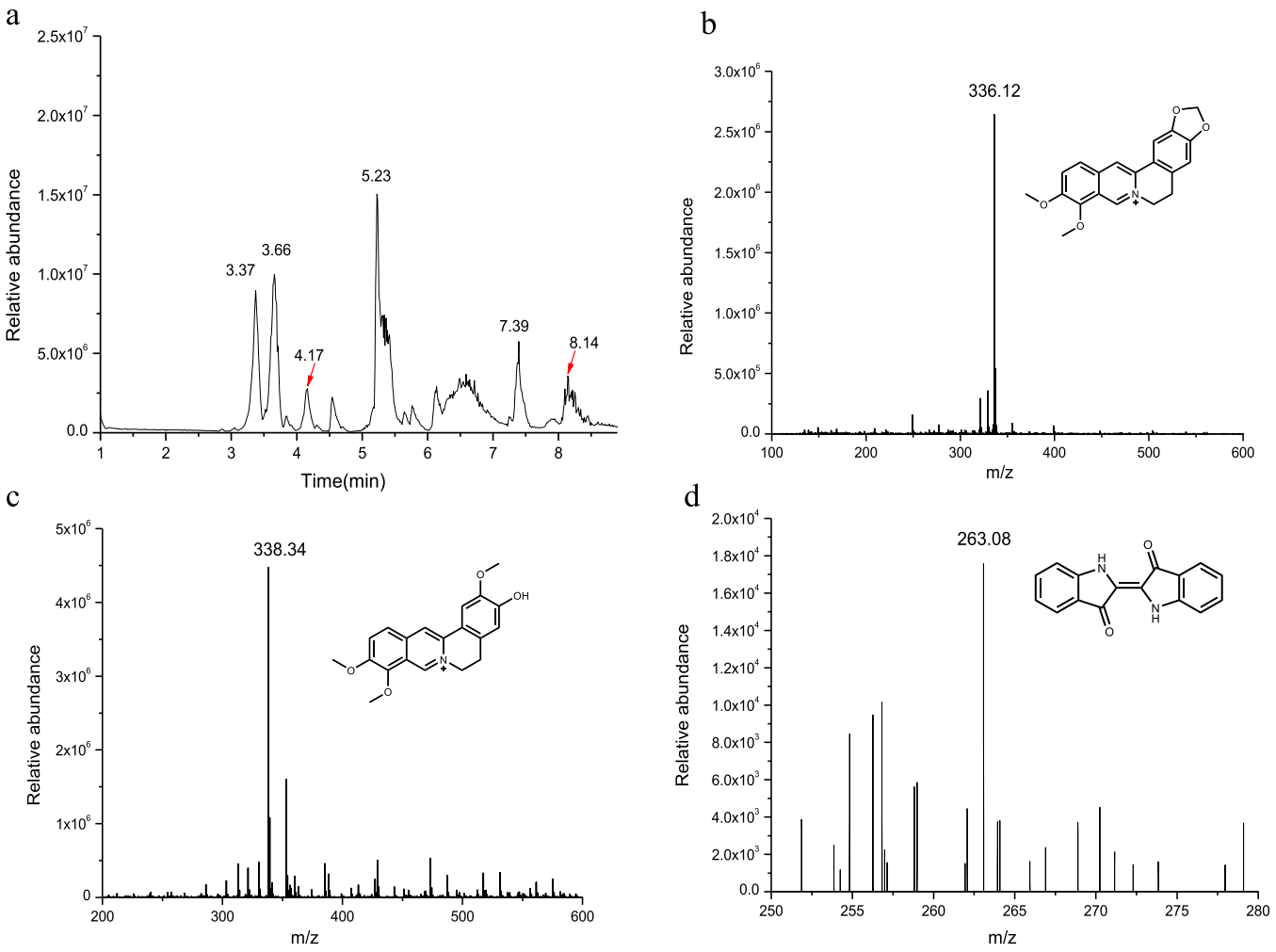

Figure 7. (a) UHPLC-Q-LTQ-Orbitrap total ion chromatogram in the purple silk extract and (b–d) MS/MS spectra of compounds m/z 336.12, m/z 338.34, and m/z 263.08 eluted in the UPLC peak at 4.22, 8.52 min, and 6.99 min, respectively, in the red silk extract.

cinnabar, the iron red was used commonly. The minium and cinnabar in the early mural have been introduced into Xinjiang from India, Afghanistan, and other Central Asian countries and then into the Central Plains.[62−64] In the middle and late Tang dynasty, cinnabar had more production in the Central Plains, and the scope of application was further expanded.[65,66]

The Raman peaks of the blue pigment at 248, 398, 767, and 831 cm^{-1} are basically consistent with the Raman peaks of azurite $[Cu_3(OH)_2(CO_3)_2]$ reference (Figure 8g). The diffraction peaks of the sample at 2θ of 17.5, 17.58, 24.72, 34.26, 40.66, and 49.26 are consistent with those of azurite $[Cu_3(OH)_2(CO_3)_2]$ (Figure 8h), indicating that there are azurite in the surface layer. In addition, the Raman peaks of the green pigment at 151.29, 176, 220.54, 267.57, and 432.10 cm^{-1} are basically consistent with the Raman peaks of malachite $[Cu_2(OH)_2CO_3]$ reference (Figure 8i). The diffraction peaks at 2θ of 18.28, 25.05, 27.62, and 34.68 are consistent with those of malachite $[Cu_2(OH)_2CO_3]$ (Figure 8j), indicating that malachite was used in the artifact. Azurite mineral is widely distributed, often together with malachite, and was used in the 4th dynasty (2900−2750 BC). Because of its wide distribution, it became one of the most widely used pigments until the start of the 19th century AD.[67,68] It was also used by the American Indians in their paintings and the Far East. Egyptians used malachite as a cosmetic as far back as the Badarian period (5000 BC). It was also found in Tutankhamun's tomb (1325 BC), probably sourced from the Sinai desert.[59] It was widely used by artists in the 16th century.

Some organic pigments have also been used in murals, pottery, and even textiles. The Raman peaks of black pigments are at 1341.7 and 1579.7 cm^{-1}, which are almost consistent with those of charcoal (Figure 8k). Carbon black is an incomplete combustion product of organic matter. Carbon black is easily prepared, and the economic cost is relatively low. In ancient times, carbon black was often used as a black pigment in Chinese ancient relics. The Raman characteristic peaks of blue pigments in murals and pottery at 259, 421, 549, 1361, and 1584 cm^{-1} are consistent with the Raman peaks of organic dye indigo reference (Figure 8l). Indigo came originally from the Caucasus in Asia; it spread to southern and central Europe and later to a wider area including Norfolk.

4. CONCLUSIONS

This work has provided a significant advancement in the origin, transmission, and exchange of the Silk Road. In this paper, in order to clarify the chemical composition of dyes and pigments in the tomb of Murongzhi, modern analysis technologies have been applied, such as Raman spectroscopy, XRD, and ultra-high-pressure liquid chromatography coupled with a thermoelectric LTQ-Orbitrap XL ETD mass spectrometer (UHPLC-MS/MS).

https://doi.org/10.1021/acsomega.2c06572
ACS Omega 2023, 8, 2508−2519

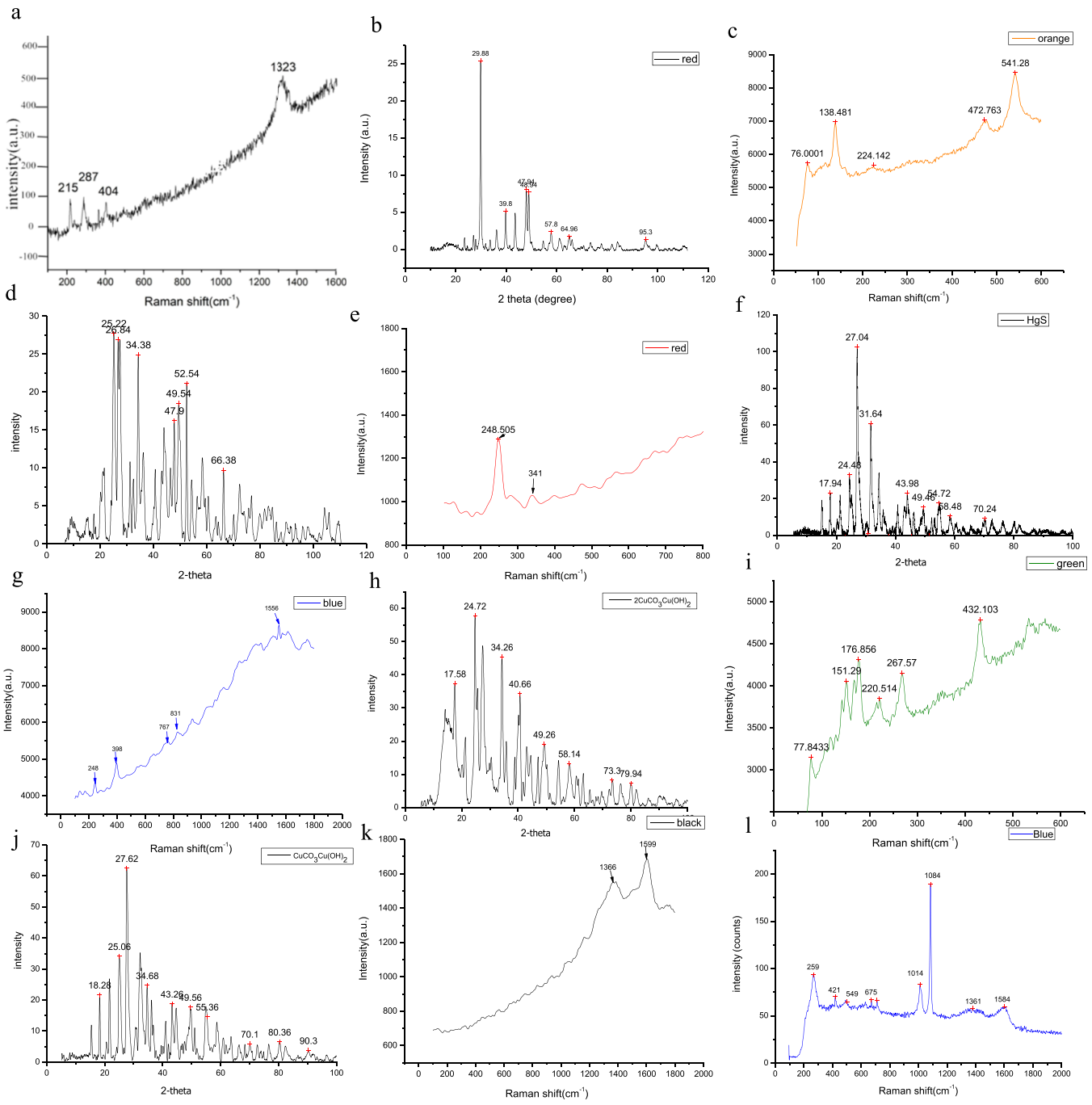

Figure 8. (a) Raman spectra of iron red (Fe_2O_3) and (b) XRD diagrams of iron red (Fe_2O_3). (c) Raman spectra of minium (Pb_3O_4) and (d) XRD diagrams of minium reference (Pb_3O_4). (e) Raman spectra of hematite (HgS) and (f) XRD diagrams of hematite (HgS). (g) Raman spectra of azurite [$Cu_3(OH)_2(CO_3)_2$] and (h) XRD diagrams of azurite [$Cu_3(OH)_2(CO_3)_2$]. (i) Raman spectra of malachite [$Cu_2(OH)_2CO_3$] and (j) XRD diagrams of malachite [$Cu_2(OH)_2CO_3$]. (k) Raman spectra of charcoal and (l) Raman spectra of indigo.

The accurate chemical composition, rubican, purpurin, berberine, jatrorrhizine, indigo, and alkannin were identified in the textile sample. Charcoal, hematite, minium, cinnabar, azurite, and malachite used as a pigment to paint the exquisite artifacts in the tomb of Murongzhi. The presence of dyes from plant and pigments from mineral suggests that the sources of various other regions became available along the Silk Road. The result indicated the influence of cultures on "Tuyuhong" in the Tang dynasty. It demonstrates that these analyses give abundant clues for learning more about the Silk Road and providing insights into cultural exchanges between the East and the West over a period of 1500 years.

■ ASSOCIATED CONTENT

Supporting Information

The Supporting Information is available free of charge at https://pubs.acs.org/doi/10.1021/acsomega.2c06572.

UV−vis spectrogram of red fibers; UV−vis spectrogram of yellow fibers; UV−vis spectrogram of blue fibers; UV−vis spectrogram of purple fibers; UV−vis spectrogram of

https://doi.org/10.1021/acsomega.2c06572
ACS Omega 2023, 8, 2508−2519

green fibers; and colorimetric evaluation of dyed samples (K/S; L^*, a^*, and b^*) (PDF)

AUTHOR INFORMATION

Corresponding Author

Guoke Chen − *Institute of Cultural Relics and Archaeology of Gansu, Lanzhou 730000, China*; Email: chenguoke1980@sina.com

Authors

Yanfei Wei − *Institute of Cultural Relics and Archaeology of Gansu, Lanzhou 730000, China*

Wenting Gu − *Institute of Cultural Relics and Archaeology of Gansu, Lanzhou 730000, China; College of Civil Engineering and Mechanics, Lanzhou University, Lanzhou 730000, China*; orcid.org/0000-0003-2980-1795

Lei Zhong − *Institute of Cultural Relics and Archaeology of Gansu, Lanzhou 730000, China*

Bingbing Liu − *Institute of Cultural Relics and Archaeology of Gansu, Lanzhou 730000, China*

Feixiang Huang − *Institute of Cultural Relics and Archaeology of Gansu, Lanzhou 730000, China*

Yuhua Chang − *Institute of Cultural Relics and Archaeology of Gansu, Lanzhou 730000, China*

Mingke Li − *Institute of Cultural Relics and Archaeology of Gansu, Lanzhou 730000, China*

Yaya Jing − *Institute of Cultural Relics and Archaeology of Gansu, Lanzhou 730000, China*

Complete contact information is available at: https://pubs.acs.org/10.1021/acsomega.2c06572

Author Contributions

Y.W. designed the experiments and wrote the manuscript. W.G. performed the data analysis for writing the article. L.Z. prepared the samples and interpreted the information of restoration of cultural relic. B.L. and F.H. revised the article. Y.C., M.L., and Y.J. provided the photographs. G.C. wrote and revised the article.

Notes

The authors declare no competing financial interest.

ACKNOWLEDGMENTS

This work was financially supported by the National Social Science Fund Key Project of Research on the Unearthed Data from the Tomb of Murongzhi (Xiwang) (project number 20AKG007), the National Cultural Heritage Administration Project of Archaeological China-Archaeology of the Tuyuhun Tombs of the Tang Dynasty, and the Gansu Provincial Cultural Relics Protection Science and Technology Research project of Application Research of Polyacrylic Acid-Functionalized Graphene/Nano-$Ca(OH)_2$ in Mural Reinforcement.

REFERENCES

(1) Liu, X. *The Silk Road in World History*; Oxford University Press, 2010.

(2) Whitfeld, S.; Sims-Williams, U. *The Silk Road: Trade, Travel, War and Faith*; Serindia Publications Inc., 2004.

(3) Sima, Q. *Records the Grant History of China (Shiji)*; Zhonghua Book Company, 1962.

(4) Liu, X. *The Silk Road in World History*; Oxford University Press, 2010.

(5) Hopkirk, P. *Foreign Devils on the Silk Road: Te Search for the Lost Cities and Treasures of Chinese Central Asia*; Oxford University Press, 2001.

(6) Beckwith, C. I. *Empires of the Silk Road: A History of Central Eurasia from the Bronze Age to the Present*; Princeton University Press, 2009.

(7) Jones, R. A. Centaurs on the silk road: Recent discoveries of Hellenistic textiles in western China. *Silk Road* **2009**, *6*, 23−32.

(8) Ge, Y.; Qi, D. *West and East: Archaeological Objects Along the Silk Roads*; Shanghai Classic Publishing House, 2017.

(9) Whitfeld, S.; Sims-Williams, U. *The Silk Road: Trade, Travel, War and Faith*; Serindia Publications Inc., 2004.

(10) Whitfeld, S. *Life Along the Silk Road*; University of California Press, 2015.

(11) Chen, G.-k.; Liu, B.-b.; Wang, S.; Zhao, Y.-j.; Wang, C.-d.; Yang, Q.-f.; Wang, Z.-y.; Zhu, A.; Han, X.-f.; Zhang, Y.-m.; et al. A Brief report on the Excavation of The Tomb of Murong Zhi during The Wu-Zhou Period in Gansu province. *Archaeol. Cultural Relics* **2021**, *2*, 15−38. (in Chinese)

(12) Liu, B.-b.; Chen, G.-k.; Sha, C.-q. On the Epitaph of Murongzhi in tang Dynasty. *Archaeol. Cultural Relics* **2021**, *02*, 87−93. (in Chinese)

(13) Tan, L.; Dong, G.; An, Z.; Edwards, R.; Li, H.; Li, D.; Spengler, R.; Cai, Y.; Cheng, H.; Lan, J.; et al. Megadrought and cultural exchange along the proto-silk road. *Sci. Bull.* **2021**, *66*, 603−611.

(14) Wouters, J. High performance liquid chromatography of anthraquinones: analysis of plant and insect extracts and dyed textiles. *Stud. Conserv.* **1985**, *30*, 119−128.

(15) Zhang, X.; Boytner, R.; Cabrera, JL.; Laursen, R. Identification of yellow dye types in Pre-Columbian Andean textiles. *Anal. Chem.* **2007**, *79*, 1575−1582.

(16) Nakamura, R.; Tanaka, Y.; Ogata, A.; Naruse, M. Dye analysis of Shosoin textiles using excitation-emission matrix fluorescence and ultraviolet-visible reflectance spectroscopic techniques. *Anal. Chem.* **2009**, *81*, 5691−5698.

(17) Berghe, I. V.; Gleba, M.; Mannering, U. Towards the identification of dyestuffs in Early Iron Age Scandinavian peat bog textiles. *J. Archaeol. Sci.* **2009**, *36*, 1910−1921.

(18) Leona, M. Microanalysis of organic pigments and glazes in polychrome works of art by surface-enhanced resonance Raman scattering. *Proc. Natl. Acad. Sci. U.S.A.* **2009**, *106*, 14757−14762.

(19) Karpova, E.; Vasiliev, V.; Mamatyuk, V.; Polosmak, N.; Kundo, L. Xiongnu burial complex: a study of ancient textiles from the 22nd Noin-Ula barrow (Mongolia, first century AD). *J. Archaeol. Sci.* **2016**, *70*, 15−22.

(20) Zhou, Z.; Shen, L.; Li, C.; Wang, N.; Chen, X.; Yang, J.; Zhang, H. Investigation of gilding materials and techniques in wall paintings of Kizil Grottoes. *Microchem. J.* **2020**, *154*, 104548.

(21) Ma, Z.; Yan, J.; Zhao, X.; Wang, L.; Yang, L. Multi-analytical study of the suspected binding medium residues of wall paintings excavated in Tang tomb, China. *J. Cult. Herit.* **2017**, *24*, 171−174.

(22) Peifan, Q.; Deqi, Y.; Qi, M.; Aijun, A.; Jingqi, Z. Study and restoration of the Yi Ma Wu Hui layer of the ancient coating on the Putuo Zongcheng Temple. *Int. J. Archit. Heritage* **2021**, *15*, 1707−1721.

(23) Wang, L.; Yang, L.; Zhou, W.; Yan, J.; Guo, R. Analysis of the techniques and materials of the colored paintings in the Renshou Hall in the Summer Palace. *Anal. Methods* **2015**, *7*, 5334−5337.

(24) Fu, Y.; Chen, Z.; Zhou, S.; Wei, S. Comparative study of the materials and lacquering techniques of the lacquer objects from Warring States Period China. *J. Archaeol. Sci.* **2020**, *114*, 105060.

(25) Hao, X.; Schilling, M.; Wang, X.; Khanjian, H.; Heginbotham, A.; Han, J.; Auffret, S.; Wu, X.; Fang, B.; Tong, H. Use of THM-PY-GC/MS technique to characterize complex, multilayered Chinese lacquer. *J. Anal. Appl. Pyrolysis* **2019**, *140*, 339−348.

(26) Karpova, E.; Nefedov, A.; Mamatyuk, V.; Polosmak, N.; Kundo, L. Multi-analytical approach (SEM-EDS, FTIR, Py-GC/MS) to characterize the lacquer objects from Xiongnu burial complex (Noin-Ula, Mongolia). *Microchem. J.* **2017**, *130*, 336−344.

(27) Hofenk, G. *The Colourful Past-origins, Chemistry and Identification of Natural Dyestuffs*; Abegg-Stiftung and Archetype Publications Ltd.: Riggisberg and London, 2004.
(28) Mouri, C.; Laursen, R. Identification of anthraquinone markers for distinguishing Rubia species in madder-dyed textiles by HPLC. *Microchim. Acta* **2012**, *179*, 105−113.
(29) Sun, G. The fiber and dye plants recorded in "The Book of Songs". *Life Word* **1987**, *6*, 36−37. (in Chinese)
(30) Duan, Y. Sino-foreign communication in southwestern China via the southern Silk Road during the Pre-Qin/Han dynasty period. *Hist. Res.* **2009**, *1*, 4−23. (in Chinese)
(31) Sun, Y. Madder-red plant dye. *Silk* **2001**, *11*, 20−22. (in Chinese)
(32) Li, W. *Study on the Extraction and Application of Red Plant Dyes*; Jiangnan University, 2007 (in Chinese).
(33) Wouters, J.; Verhecken, A.; Verhecken, A. The coccid insect dyes: HPLC and computerized diodearray analysis of dyed yarns. *Stud. Conserv.* **1989**, *34*, 189−200.
(34) Shao, H. The research of Zaghunluq culture in Xinjiang. *Res. China Front Archaeol.* **2008**, *7*, 170−183. (in Chinese)
(35) Liu, J.; Zhao, F. Dye analysis of two polychrome woven textiles from the Han and Tang dynasties. In *Color in Ancient and Medieval East Asia*; Dusenbury, M. M., Ed.; Yale University Press: New Haven and London, 2015; pp 113−119.
(36) Zhang, X.; Good, G.; Laursen, L. Characterization of dyestuffs in ancient textiles from Xinjiang. *J. Archaeol. Sci.* **2008**, *35*, 1095−1103.
(37) Surowiec, I.; Szostek, B.; Trojanowicz, M. HPLC-MS of anthraquinoids, flavonoids, and their degradation products in analysis of natural dyes in archeological objects. *J. Sep. Sci.* **2007**, *30*, 2070−2079.
(38) Petroviciu, I.; Teodorescu, I.; Albu, F.; Virgolici, M.; Nagoda, E.; Medvedovici, A. Dyes and biological sources in nineteenth to twentieth century ethnographic textiles from Transylvania, Romania. *Heritage Sci.* **2019**, *7*, 1−15.
(39) Ahn, C.; Zeng, X.; Li, L.; Obendorf, S. K. Thermal degradation of natural dyes and their analysis using HPLC-DAD-MS. *Fash. Text.* **2014**, *1*, 22.
(40) Tamburini, D. Investigating Asian colourants in Chinese textiles from Dunhuang (7th−10th century AD) with high performance liquid chromatography tandem mass spectrometry-Towards the creation of a mass spectra database. *Dyes Pigm.* **2019**, *163*, 454−474.
(41) Yang, L.; Ye, M.; Gao, S. Based on the revision of pharmacopoeia of the People's Republic of China on the study of the main effective components of phellodendron. *China J. Tradit. Chin. Med. Pharm.* **2018**, *33*, 3905−3908. (in Chinese)
(42) Fu, L.; Hong, T. *Higher Plants of China*; Qingdao Publishing House, 2001; p 425 (in Chinese).
(43) Liu, J.; Mouri, C.; Laursen, R.; Zhao, F.; Zhou, Y.; Li, W. Characterization of dyes in ancient textiles from Yingpan, Xinjiang. *J. Archaeol. Sci.* **2013**, *40*, 4444−4449.
(44) Jing, Y.; Xun, Z.; Guang, Z. L.; Xue, R. Ultra-high performance liquid chromatography-photodiode array detector-tandem mass spectrometry to analyze blue dyes in She ethnic clothing. *J. Text. Res.* **2019**, *40*, 128−135. (in Chinese)
(45) Garcia-Macias, M.; John, P. Formation of natural indigo derived from woad (Isatis tinctoria L.) in relation to product purity. *J. Agric. Food Chem.* **2004**, *52*, 7891−7896.
(46) Mantzouris, D.; Karapanagiotis, I.; Panayiotou, C. Comparison of extraction methods for the analysis of Indigofera tinctoria and Carthamus tinctorius in textiles by high performance liquid chromatography. *Microchem. J.* **2014**, *115*, 78−86.
(47) Splitstoser, J.; Dillehay, T.; Wouters, J.; Claro, A. Early pre-Hispanic use of indigo blue in Peru. *Sci. Adv.* **2016**, *2*, 1501623.
(48) Assimopoulou, A.; Karapanagiotis, I.; Vasiliou, A.; Kokkini, S.; Papageorgiou, V. Analysis of alkannin derivatives from Alkanna species by high-performance liquid chromatography/photodiode array/mass spectrometry. *Biomed. Chromatogr.* **2006**, *20*, 1359−1374.
(49) Han, J.; Weng, X.; Bi, K. Antioxidants from a Chinese medicinal herb−Lithospermum erythrorhizon. *Food Chem.* **2008**, *106*, 2−10.
(50) Liu, J.; Guo, D.; Zhou, Y.; Wu, Z.; Li, W.; Zhao, F.; Zheng, X. Identification of ancient textiles from Yingpan, Xinjiang, by multiple analytical techniques. *J. Archaeol. Sci.* **2011**, *38*, 1763−1770.
(51) Cardon, D. *Natural Dyes: Sources, Tradition, Technology and Science*; Archetype Publications Ltd.: London, 2007.
(52) Bai, X. Research on identification technology of plant dyes for silk fabrics unearthed in humid tomb environment. Doctoral Dissertation; University of Science and Technology of China, 2014 (in Chinese).
(53) Garcia-Macias, M.; John, P. Formation of natural indigo derived from woad (Isatis tinctoria L.) in relation to product purity. *J. Agric. Food Chem.* **2004**, *52*, 7891−7896.
(54) Chen, Y.; Xie, Y.; Xiong, Y. Study on the analysis and identification of blue dyes on woolen fabrics unearthed from the Zhagunluke Tombs. *Shanghai Mus. J.* **2000**, *8*, 677−684. (in Chinese)
(55) Sun, Y. Madder-red plant dye. *Silk* **2001**, *11*, 20−22. (in Chinese)
(56) Berghe, I. V.; Gleba, M.; Mannering, U. Towards the identification of dyestuffs in Early Iron Age Scandinavian peat bog textiles. *J. Archaeol. Sci.* **2009**, *36*, 1910−1921.
(57) Zhang, L.; Tian, K.; Wang, Y.; Zou, J.; Du, Z. Characterization of Ancient Chinese Textiles by ultra-high performance liquid chromatography/quadrupole-time of flight mass spectrometry. *Int. J. Mass Spectrom.* **2017**, *421*, 61−70.
(58) Liu, J.; Mouri, C.; Laursen, R.; Zhao, F.; Zhou, Y.; Li, W. Characterization of dyes in ancient textiles from Yingpan, Xinjiang. *J. Archaeol. Sci.* **2013**, *40*, 4444−4449.
(59) Abel, A. The history of dyes and pigments: From natural dyes to high performance pigments. *Colour Design*; Elsevier, 2012; pp 557−587.
(60) Lucas; European Microbeam Analysis Society (EMAS). *Microchimica Acta*; Science Press, 2017; pp 22−27 (in Chinese).
(61) Xia, Y. *Chinese Historical Pigments in Polarized Light Microscope*; Science Press: Beijing, 2017; pp 22−27 (in Chinese).
(62) Su, B.; Hu, Z.; Li, Z. A study of the mixed pigments used in the wall painting of Dunhuang. *Dunhuang Res.* **1996**, *3*, 149−162. (in Chinese)
(63) Argote, D. L.; Torres, G.; Hernández-Padrón, G.; Ortega, V.; López-García, P. A.; Castaño, V. M. Cinnabar, hematite and gypsum presence in mural paintings in Teotihuacan Mexico. *J. Archaeol. Sci.* **2020**, *32*, 102375.
(64) Antunes, V.; Candeias, A.; Oliveira, M. Characterization of gypsum and anhydrite ground layers in 15th and 16th centuries Portuguese paintings by Raman Spectroscopy and other techniques. *J. Raman Spectrosc.* **2014**, *45*, 1026−1033.
(65) La Spina, V.; Grau Giménez, G.; Carles, J. Uses of gypsum in Spanish architectural heritage: typologies and some unique. *Int. J. Archit. Heritage* **2020**, *14*, 176−195.
(66) Garrote, M.; Robador, M.; Perez-Rodriguez, J. Analytical investigation of Mudéjar polychrome on the carpentry in the Casa de Pilatos palace in Seville using non-destructive XRF and complementary techniques. *Spectrochim. Acta, Part A* **2017**, *173*, 279−291.
(67) Chen, G.; Yu, Z.; Chai, B.; Cui, Q.; Zhang, W.; Wang, X.; Peng, F. On the application of nondestructive in situ analysis on wall paintings of the Lu Tusi Yamen building in Yongdeng County. *Dunhuang Res.* **2018**, *169*, 28−37.
(68) Wang, J.; Li, J.; Tang, J.; Xu, Z. Study on mural pigment of Qutan temple in Qinghai province. *Sci. Conserv. Archaeol.* **1993**, *5*, 23−35.

https://doi.org/10.1021/acsomega.2c06572
ACS Omega 2023, 8, 2508−2519